Clim. Past Discuss., 11, 1479–1518, 2015
www.clim-past-discuss.net/11/1479/2015/
doi:10.5194/cpd-11-1479-2015

Climate of the Past
Discussions
Open Access

Variability of daily winter wind speed distribution over Northern Europe during the past millennium in regional and global climate simulations

S. E. Bierstedt[1], B. Hünicke[1], E. Zorita[1], S. Wagner[1], and J. J. Gómez-Navarro[2]

[1]Institute of Coastal Research, Helmholtz-Zentrum Geesthacht, Geesthacht, Germany
[2]Climate and Environmental Physics, Physics Institute and Oeschger Centre for Climate Change Research, University of Bern, Switzerland

Received: 12 March 2015 – Accepted: 15 April 2015 – Published: 29 April 2015

Correspondence to: S. E. Bierstedt (svenja.bierstedt@hzg.de)

Published by Copernicus Publications on behalf of the European Geosciences Union.

Abstract

We analyse the variability of the probability distribution of daily wind speed in wintertime over Northern and Central Europe in a series of global and regional climate simulations covering the last centuries, and reanalysis products covering approximately the last 60 years. The focus of the study lies in identifying the link between the variations in the wind speed distribution to the regional near-surface temperature, to the meridional temperature gradient and to the North Atlantic Oscillation.

The climate simulations comprise three simulations, each conducted with a global climate model that includes a different version of the atmospheric model ECHAM. Two of these global simulations have been regionalised with the regional climate models MM5 and CCLM. The reanalysis products are the global NCEP/NCAR meteorological reanalysis version 1 and a regional reanalysis conducted with a regional atmospheric model driven at its domain boundaries by the NCEP/NCAR reanalysis.

Our main result is that the link between the daily wind distribution and the regional climate drivers is strongly model dependent. The global models tend to behave similarly, although they show some discrepancies. The two regional models also tend to behave similarly to each other, but surprisingly the results derived from each regional model strongly deviates from the results derived from its driving global model. The links between wind speed and large-scale drivers derived from the reanalysis data sets overall tend to resemble those of the global models. In addition, considering multi-centennial time scales, we find in two global simulations a long term tendency for the probability distribution of daily wind speed to widen through the last centuries. The cause for this widening is likely the effect of the deforestation prescribed in these simulations.

We conclude that no clear systematic relationship between the mean temperature, the temperature gradient and/or the North Atlantic Oscillation, with the daily wind speed statistics can be inferred from these simulations. The understanding of past and future changes in the distribution of wind speeds, and thus of wind speed extremes, will re-

CPD
11, 1479–1518, 2015

quire a detailed analysis of the representation of the interaction between large-scale and small-scale dynamics.

1 Introduction

Anthropogenic climate change is expected to cause an increase of various types of extreme events, such as heat waves, but its effects on extreme winds is less clear. Section 3 of the Intergovernmental Panel on Climate Change (IPCC) special report "Managing the Risks of Extreme Events and Disasters to Advance Climate Change Adaptation" states that there is only low confidence in projections of changes in extreme winds (Seneviratne et al., 2012). One way to reduce this uncertainty is to compare the output of paleoclimate simulations over the past centuries with empirical evidence of past wind conditions, for instance derived from historical evidence or natural proxies (Costas, 2013). While there is still a dearth of proxy records reflecting past changes in wind speed, new types of proxy records are being developed (Costas, 2013). A precondition for this comparison is to test whether different climate models provide a consistent picture of past changes in wind speed distribution. In this study we analyse several simulations with global and regional models and investigate to what extent they provide a consistent view of the relationship between the variations in the wind speed distribution and large-scale drivers. We focus on Northern Europe in wintertime as this region and season are particularly prone to storminess.

Hypotheses put forward to explain changes in storminess are related to the general physical consideration that warmer periods provide more humidity and consequently more (latent) energy for possible storms. However, warmer periods are generally characterized by a weaker meridional temperature gradient due to the stronger warming of the high latitudes with respect to the tropics, and thus a weaker baroclinicity, which should lead to weaker or less storms (Li and Woollings, 2014; Yin, 2005). In addition, the North Atlantic Oscillation (NAO), as the main pattern of troposphere dynamics over the North Atlantic-European sector, is also related to the interannual variability

CPD
11, 1479–1518, 2015

of seasonal mean winds in this region. It is thus very plausible that it is also involved in the variations of the distribution of daily wind speeds. The NAO itself could also be related to changes in temperature. In this regard, scenario simulations in general indicate a tendency towards a stronger meridian pressure gradient in the future (Gillett and Fyfe, 2013), but the link between the NAO and external climate forcing over the past centuries is unclear in climate simulations (Gómez-Navarro and Zorita, 2013).

Thus, from the dynamical point of view it is not clear how the distribution of wind speed would respond to changes in temperature. The analysis of long-term trends in wind extremes and storminess in the observational record has so far yielded inconclusive results, probably due to the difficulty of constructing homogeneous series of wind speed, because of e.g. station relocation or changing measuring techniques. On the other hand, reanalysis products covering long periods (e.g. the 20th Century Reanalysis 20CR, Compo et al., 2011) may be inhomogeneous due to the assimilation of new types of data through the simulated period. There has been a considerable debate on the storminess trends in long-term reanalysis data sets (Brönnimann et al., 2012; Krueger et al., 2013; Wang et al., 2013). Krueger et al. (2013) stated that before 1950 the time series of 20CR and observational mean sea level pressure are not consistent. They suggested that the increasing station density leads to these inconsistencies. Wang et al. (2013), on the other hand, argued that new measurement errors and changed sampling frequencies would produce these inhomogeneities. This debate has also been discussed by Feser et al. (2014), who concluded that the analysis of long-term reanalysis data, affected by changing station density, should be conducted with caution.

The analysis of the climate of the past centuries can shed light on the question whether external climate forcing has an effect on the intensity or frequency of wind extremes and whether or not the temperature variability is linked to variability in statistics of wind speeds. Unfortunately, proxy-based climate reconstructions in general still do not provide information about extreme wind statistics in the past, except for intense tropical cyclones (e.g. Donnelly and Woodruff, 2007). However, new types of proxy data

CPD
11, 1479–1518, 2015

that may record past wind speed are being retrieved. For instance, coastal dunes at the North Sea coast contain layered structures that can be analysed by ground-penetrating radar. The layered structures contain information about grain size distribution and, indirectly, about intensity or frequency of high winds in the past (Costas, 2013). These types of proxies can potentially be used to test the skill of climate models to simulate the relationships between extreme wind statistics and external forcing or between extreme wind statistics and low-frequency variability of the large-scale surface climate.

The evolution of temperatures of the past millennium in this region, as reconstructed from proxy and long-instrumental records, exhibits a generally warm period in the early centuries (the Medieval Warm Period) and generally colder centuries around 1700 AD (the Little Ice Age), with the subsequent warming leading to the current recent warm period (Luterbacher et al., 2004; 2k Consortium, 2013; Esper et al., 2014). This alternation of warm and cold periods has been likely caused by external climate forcings (Hunt, 2006; Fernández-Donado et al., 2013), in particular the recent warm period and the Little Ice Age, and thus it provides a suitable test of whether the variability of extreme wind statistics may follow a similar alternation.

Climate simulations had been previously used to address the connection between winds and temperatures in the past (e.g. Fischer-Bruns et al., 2005; Schimanke et al., 2012). Fischer-Bruns et al. (2005) analysed two historical climate simulations with the global climate model ECHO-G covering the period from 1550 to 1990 AD. These authors found that storminess and large-scale temperature variations were mostly decoupled in these simulations. However, they mentioned a connection between storm track variability and temperature over the North Atlantic for one of the two simulations in two periods with extremely low external forcing, namely the Late Maunder Minimum (1675–1710 AD) and the Dalton Minimum (1790–1840 AD). Nevertheless, they found no evidence of a linear co-variation between the number of extra-tropical storms and temperature variations in the simulations analysed.

However, the spatial resolution of global climate models may not be adequate to realistically represent extreme events, especially over regions with complex coastlines. Re-

CPD
11, 1479–1518, 2015

gional climate models, driven by the fields simulated by global climate models, should provide a better representation of small-scale processes and of the land–sea contrasts (Hall, 2014), and thus they should be better suited for the simulation of extreme events. Nevertheless, despite the fact that regional models provide an added value (Feser et al., 2011) they are also bound by the circulation biases of the driving global climate model simulations (Hall, 2014).

In this study we present an analysis of the variability of daily wind speed statistics over Northern Europe over the past centuries as simulated by different climate models. We mainly focus on the consistency among the different models in simulating the relationship between large-scale drivers and the statistics of daily wind speed with the goal of identifying robust patterns across models that can be later tested with proxy reconstructions. Our main result indicates that climate models provide still ambiguous answers, which should be reconciled first.

This paper is structured as follows: Section 2 describes the analysed data sets separated into climate simulations of global circulation models, regional circulation models and reanalysis products. Section 3 defines our area of interest and outlines the applied methods and definitions. Section 4 presents the analysis of the relationship of large-scale drivers and wind speed variance, as well as the comparison of the evolution of the wind speed variance in the millennium simulations. A discussion of the results and conclusions closes the manuscript.

2 Data

Our study focuses on the statistical relationship between mean temperature/pressure and daily wind statistics. We use monthly mean two-meter temperature (T2M) values, monthly mean values of mean sea level pressure (MSLP) and daily mean 10 m wind speed (WS) for our analysis. These values are taken from a set of five simulations performed with five different models, with different spatial and temporal resolution: two simulations with the Regional Climate Models (RCMs) MM5 and CCLM, and three

CPD
11, 1479–1518, 2015

simulations with the global General Circulation Models (GCMs) ECHAM4-HOPE-G, ECHAM5/MPI-OM and ECHAM6/MPI-OM. ECHAM4-HOPE-G and ECHAM5-MPIOM were chosen because they had been used as the boundary forcing for the two RCM simulations, respectively. ECHAM6/MPI-OM was chosen due to its higher spatial resolution similar to the resolution of the RCM simulations analysed, but also for being the next generation of the previous versions of ECHAM4 and ECHAM5. Additionally, we analyse the global reanalysis NCEP/NCAR version 1 and the regional reanalysis coastDat2. Table 1 summarizes the information about spatial and temporal resolution and time periods of the data sets used. In the following we introduce the different data sets in more detail and describe their differences.

2.1 Global Climate Model simulations

The coupled GCM ECHAM4-HOPE-G, also denoted in previous literature as ECHO-G (Legutke and Voss, 1999) consists of the atmospheric component (AGCM) ECHAM4 (Roeckner et al., 1996) and the ocean-ice component (OGCM) HOPE-G (Wolff et al., 1997). ECHAM4 has a horizontal resolution of T30 (approx. $3.75^\circ \times 3.75^\circ$, $\approx 400\,\text{km} \times 260\,\text{km}$ in high mid-latitudes) and 19 vertical levels and HOPE-G a horizontal resolution corresponding to T42 (approx. $2.8^\circ \times 2.8^\circ$, $\approx 300\,\text{km} \times 200\,\text{km}$ in high mid-latitudes) and 20 vertical levels. Both sub-models have been developed at the Max Planck Institute for Meteorology (MPI-M) in Hamburg. The analysed ECHO-G millennium simulation (1001–1990 AD) is part of an ensemble of simulations conducted by the Helmholtz-Zentrum Geesthacht (HZG). The simulation is forced with changes in total solar irradiance, the dimming effect of volcanic eruptions on solar irradiance, and changes in greenhouse gases (CO_2, NO_2, CH_4). The simulation was started with a cold ocean initial condition taken from a previous simulation corresponding to a situation representative of the Little Ice Age (Hünicke et al., 2011; von Storch et al., 2004; Zorita et al., 2004).

The coupled GCM ECHAM5/MPI-OM consists of the atmospheric component ECHAM5 (successor of ECHAM4, Roeckneret al., 2003) and the ocean and sea-ice component MPI-OM (Marsland et al., 2003). ECHAM5 has a T31 resolution with 31 vertical levels. The MPI-OM component has a horizontal resolution corresponding to T42 and 23 vertical levels. The analysed simulation ECHAM5/MPI-OM (850–2005 AD) is part of an ensemble of simulations conducted by the Max-Planck-Institute for Meteorology in Hamburg and will hereafter simply be named ECHAM5. It is driven by changes in solar irradiance (Krivova and Solanki, 2008), volcanic eruptions (Crowley et al., 2008), changes in earth' orbital parameters, greenhouse gas and aerosol forcings. Additionally, land cover changes (Pongratz et al., 2008) are considered in this simulation. More details about the simulation setup and forcings can be found in Jungclaus et al. (2010).

We also include a climate simulation with the model MPI-ESM with the P configuration (MPI-ESM-P, Giorgetta et al., 2013), which consist of the successor of ECHAM5 and the newest version of ECHAM, named ECHAM6 (850–2005 AD). The main differences between ECHAM6 and ECHAM5 are the higher vertical resolution (i.e., 47 instead of 31 vertical levels), increased horizontal resolution of T63 ($1.875^{\circ} \times 1.875^{\circ}$, $\approx 200\,\text{km} \times 130\,\text{km}$ in high mid-latitudes), the incorporation of new aerosol and surface albedo climatology and the use of a new shortwave radiation scheme in ECHAM6 (Crueger et al., 2013). The MPI-ESM-P simulation is part of the Climate Model Intercomparsion Project version 5 (CMIP5, Taylor et al., 2012). The boundary layer and turbulence parametrization in ECHAM6 is based on the eddy diffusivity/viscosity approach (Stevens et al., 2013). The model was driven by changes in greenhouse gases and spectrally resolved solar irradiance, volcanic activity (Crowley et al., 2008), changes in earth' orbital parameters and land use changes (Pongratz et al., 2008). Note that ECHAM5 and ECHAM6 are the only simulations included in this analysis forced with land use changes.

2.2 Regional Climate Model simulations

The RCM MM5 model consists of a slight modification of the non-hydrostatic Fifth-generation Pennsylvania-State University-National Center for Atmospheric Research

CPD
11, 1479–1518, 2015

Mesoscale Model. Such modification allows this meteorological model to perform long climate simulations. This setup has been used to conduct a long high-resolution climate simulation of the European climate during the last millennium, driven at the domain boundaries by the coupled GCM ECHO-G (Gómez-Navarro et al., 2013, 2015). For the planetary boundary layer formation parametrization, this simulation uses the medium-range forecast (MRF, Hong and Pan, 1996) scheme. The RCM was driven by the same set of external forcing as the driving GCM ECHO-G (see Sect. 2.1) to avoid physical inconsistencies. MM5 has a spatial resolution of $0.5^{\circ} \times 0.5^{\circ}$ ($\approx 70\,\text{km} \times 40\,\text{km}$). The model output is available on a daily scale and covers the period 1001–1990 AD. The analysed millennium simulation MM5-ECHO-G will hereafter be named MM5.

A second regional simulation is carried out with the non-hydrostatic operational weather prediction model COSMO in CLimate Mode (CCLM) (Rockel and Hense, 2008). The CCLM model is driven by initial and boundary conditions of the global ECHAM5 simulation. The regional model is, however, free to produce its own small scale spatial variability. The COSMO model uses a boundary layer approximation by implying horizontal homogeneity of variables and fluxes, which ignores all horizontal turbulent fluxes (Doms et al., 2011). The CCLM simulation over Europe has roughly the same spatial resolution as the MM5 simulation, but it covers only the period from 1655 to 1999 AD. The simulation CCLM-ECHAM5 will hereafter be abbreviated as CCLM.

2.3 Reanalysis data

The NCEP/NCAR reanalysis covers the period from 1948-present and has a spatial resolution of 2.5° ($\approx 270\,\text{km} \times 175\,\text{km}$ in high mid-latitudes) with 28 levels and is available at 6 hourly intervals (Kalnay et al., 1996; Kistler et al., 2001). In addition we analyse the high resolution regional product coastDat2 (Geyer, 2014) resulting from a simulation with the regional model CCLM and driven by the global NCEP/NCAR reanalysis using also the same spectral nudging technique (after von Storch et al., 2000). The regional reanalysis coastDat2 covers Europe and the North Atlantic for the period from 1948 to present. It has a spatial resolution of 0.22° ($\approx 25\,\text{km} \times 15\,\text{km}$) and the output is

CPD
11, 1479–1518, 2015

available on hourly time intervals. This data set will be denoted in the following coastDat2.

All wind speed data were daily averaged to proceed with the analysis.

3 Methods and definitions

Our analysis concentrates on the distribution of daily wind speed in wintertime (December, January, February – DJF) over central and northern Europe. The area of investigation has approximately the same extension from 45 to 65° N and 0 to 30° E for all data sets analysed.

The statistics of daily wind speed were evaluated over gliding time for the different simulation periods. These wind speed statistics include the STD of the distribution, its 50th, 95th and 99th percentiles (P50, P95, P99) and the differences P95 minus P50 (diffM) and P99 minus P95 (diffE) as a measure of the width of the distribution in the high wind ranges. The analysis of several percentiles and their differences allows the determination of basic changes in the characteristics of wind speed distributions, hence it is possible to investigate if it shifts with time with unchanged shape and/or whether its width changes. The three climate parameters analysed regarding their influence on wind speed are (1) mean seasonal near-surface air temperature (mTemp), (2) mean seasonal meridional temperature gradient (tGrad) and (3) the North Atlantic Oscillation index (NAO).

Because we are interested in the relationship between the slowly changing mean climate and the variability of the distribution of daily wind speed, the wind statistics are calculated considering gliding time windows over the respective time series for each model simulation. The climate parameters analysed are considered as means over the respective time windows. For the long climate model simulations (ECHO-G, ECHAM5, ECHAM6, MM5, CCLM) we use 30 year running windows and for the shorter reanalysis data (coastDat2, NCEP) 5 year running time windows.

The temperature gradient is calculated as the absolute value of the difference between the northern (N) and the southern (S) half of the investigation area tGrad = abs(N – S) for each model simulation.

The North Atlantic Oscillation (NAO) index is defined as the leading pattern resulting from principal component analysis (PCA) of the winter mean sea-level pressure (MSLP) field. This dominant pattern of variability is characterized in all simulations by a low pressure system over Iceland and a high pressure system over the Azores.

3.1 Test for significance: random-phase bootstrap

A random-phase bootstrap method (Schreiber and Schmitz, 1996; Ebisuzaki, 1997) is applied to determine the significance of the correlation coefficients shown in Table 2 with a significance level of $p = 0.05$. This method allows us to take into account the autocorrelation structure of the series. For this method a Fourier transformation of the time series is conducted. The phases of the Fourier-transformed series are then replaced by random phases, and the result is transformed back to the time domain to obtain new surrogate time series. The surrogate time series has the same spectrum and autocorrelation as the original time series, but has a random time evolution. By generating a large number of surrogate time series, an empirical distribution of the correlation coefficient under the null-hypothesis (that the correlation is zero) can be constructed and used to determine the statistical significance of the correlation coefficient.

4 Results

As previously mentioned, this study is based on correlations between different parameters of the probability distribution of daily mean wind in wintertime and selected potential drivers: mean seasonal near-surface air temperature (mTemp), mean seasonal meridional temperature gradient (tGrad) and North Atlantic Oscillation index (NAO). Table 2 presents a summary of the statistical relationships derived from the different

CPD
11, 1479–1518, 2015

model simulations analysed. The presented time correlation coefficients are obtained by calculating the parameters of the daily wind probability distribution at grid-cell scale, followed by averaging over the whole spatial domain. The spatially resolved statistical analysis is presented for each model in the following sections. The significance of the correlation coefficients presented in Table 2 is tested as described in Sect. 3.1 by a random phased bootstrap method and marked as bold characters.

In the following, we first present the general findings for each of the climate drivers analysed (mTemp, tGrad, NAO) by comparing all considered model simulations and reanalysis products. This is followed by a more detailed presentation of the results with focus on (a) the regional model simulations and their corresponding driving global models (b) the simulation with the global model ECHAM6/MPI-OM and (c) the reanalysis products. In addition, for some of the long simulations a comparison of time slices is presented.

4.1 General comparison of all data sets

4.1.1 Relationship between mTemp and tGrad

A common characteristic shared by all analysed simulations is the negative correlation between the mean winter temperature (mTemp) and the mean meridional temperature gradient (tGrad). Hence, in warmer decades the northern regions warm more strongly than the southern regions, and in colder decades the northern regions also cool more strongly than the southern regions. This “high-latitude amplification” is also found in climate simulations for future scenarios. In those simulations, it is caused by several positive feedbacks that operate more strongly at high latitudes, such as ice-snow-albedo feedback (Hall and Qu, 2006) and black-body radiation feedback (Pithan and Mauritsen, 2014). European temperature reconstructions over the past centuries also indicate that in colder periods such as the Late Maunder Minimum (around 1700 AD) temperatures in higher latitudes cooled down more strongly than further south (Luterbacher et al., 2002).

4.1.2 Relationship between mTemp and wind speeds

The relationship between the mTemp and the median winds (P50) is positive in all analysed simulations and reanalysis products, with the exception of the regional simulation with MM5. The correlations, taken individually, are not always statistically significant at the 5 % level. These positive correlations imply that periods with higher winter temperatures than normal also tend to show higher median winds. Contrary to the rest of the simulations and also opposite to the link found in its driving global model ECHO-G, the behavior of the regional model MM5 is not limited to this particular correlation between mean air temperature and median wind. Table 2 already shows that the MM5 simulation often behaves differently compared to all other simulations. The other regional model CCLM does show a positive correlation between air temperature and median wind, but this correlation is lower compared to the global simulations and in the reanalysis products.

Warmer air temperatures are also strongly linked to larger values of the high percentiles of the distribution of daily wind, P90 and P95, for most of the simulations. Again, the exceptions relate to the regional model simulations MM5 and CCLM. MM5 presents a negative correlation and CCLM a weak positive correlation.

Variations in the width of the daily wind distribution are described by the differences between the high percentiles, P90 or P95, and the median wind P50. The correlations between these measures of the distribution widths and mean temperature tend to be small for all simulations with the exceptions of the regional models MM5 and CCLM. For these two regional models the correlations are strongly negative, and more strongly so for the MM5 model, indicating that in periods with warmer air temperatures the wind distribution gets narrower at the same time that it shifts to lower values of wind speed, as indicated by the negative correlation with P50.

CPD
11, 1479–1518, 2015

4.1.3 Relationship between tGrad and wind speeds

The correlation coefficients between the distribution of wind speeds and tGrad are summarized in the second block of Table 2. In general, the correlations tend to be weak, with some exceptions. In the MM5 simulations they are stronger and positive, whereas in the ECHAM6 simulation they are somewhat weaker but negative. Both reanalysis products also offer a contrasting picture. In the NCEP reanalysis the correlations between tGrad and the median wind P50 or the higher percentile winds P90 and P95 are negative and statistically significant, whereas in the coastDat2 product they tend to be positive but weak.

4.1.4 Relationship between NAO and wind speeds

The NAO is a large-scale winter circulation pattern that describes the mean strength of the seasonal mean westerly winds in the North Atlantic-European sector and therefore it is plausible that it is also related to the distribution of the daily wind speed in Northern Europe. The correlations between the NAO index across the different simulations yield, however, an incoherent picture. Most simulations display a positive and relatively strong correlation between the NAO index and the spatially averaged P50, with the exception of the two regional models, MM5 and CCLM.

Thus, the regional models behave again different to their respective driving GCMs. In the case of MM5 the correlation between the NAO index and P50 correlation is strikingly negative whereas in the case of CCLM the correlation is weakly positive. A positive phase of the NAO is linked to stronger westerly winds over Northern Europe and hence a negative or weakly negative correlation of the NAO with P50 is surprising. We show later that the negative sign of this correlation in the regional simulations is caused by the behavior of the regional models over land areas, whereas the sign of the correlation over ocean is the expected one.

The correlation between the NAO index and the width of the distribution (STD) of wind speed averaged over the study region tends to be also positive for most simula-

CPD
11, 1479–1518, 2015

tions, indicating that stronger mean westerlies tend to concur with a wider distribution of daily wind speed. However, there are exceptions. Again, the regional model simulation MM5 displays a strong negative correlation and the regional model simulation CCLM shows a positive but weak correlation. These negative (MM5) or positive but weak (CCLM) correlations also contrast with the link between the NAO index and the width of the wind speed distribution in their parent global models, ECHO-G and ECHAM5, respectively, both of which display positive and statistically significant correlations. Similarly to the global models, in both reanalysis products the NAO index is strongly and positively correlated with the width of the wind speed distribution.

4.1.5 Relationship between NAO and mTemp

It is well known that the winter NAO index is positively correlated with air temperatures in Northern Europe. The link between the parameters of the wind speed distribution on one side, and the NAO or the mean air temperature on the other side may thus be just a reflection of the same physical relationship. This is also supported by paying attention to how the correlations with the NAO and with the mean temperature vary across simulations (last two lines in Table 2). It seems clear that both lines in the table display a similar, though not identical, pattern of correlations across the simulations analysed. However, the spatially aggregated analysis does not allow to disentangle which of both factors, NAO or mTemp, is the physical driving factor for the variations in the distribution of wind speed.

4.1.6 Relationship between mTemp, tGrad and wind speed

The correlations shown in Table 2 are indicative of a simple relationship between mTemp or tGrad on one side and median wind speed or the width of its probability distribution on the other side. Certainly, there must be other underlying factors that require a more detailed analysis. For instance, the period covered by the different data

CPD
11, 1479–1518, 2015

products is different. The reanalysis products represent the last decades, when the anthropogenic warming is probably dominating temperature trends.

In the following subsections we investigate in more detail the links between the large-scale atmospheric drivers and the distributions of daily wind at a grid-cell level, which allows us to better understand the spatially aggregated correlations included in Table 2. The following figures (Figs. 1–4) display the correlation patterns between the different large-scale climate indices and the parameters of the wind speed distribution at grid-cell scale. The upper two panels in the figures show the results derived from the regional models for direct comparison with their driving GCMs. The lower two panels include the results derived from the GCM ECHAM6 (not used to drive any regional model in this study) and the two reanalysis products.

4.2 Simulations of the regional models CCLM and MM5 vs. their driving global models ECHAM5 and ECHO-G

In the CCLM simulation (1655–1999 AD) the relationship between P50 wind speed and mTemp in general shows a negative correlation or correlations close to zero, with the exception of a land area east of the Baltic where the correlation is positive (Fig. 1). Hence, in this regional simulation, colder periods can be related to generally stronger winds. In contrast, the correlation between the mean temperature and P50 in the ECHAM5 simulation is positive almost everywhere, with some regions showing lower correlations. The MM5 and the ECHO-G simulations also display a qualitatively similar, but even more clear, contrast. In the MM5 simulation, median wind speeds over land areas are clearly negatively correlated with mean temperature, whereas over oceanic areas P50 is positively correlated with mTemp. The ECHO-G simulation displays clearly positive correlations over the whole area, similar to the ECHAM6 simulation and the regional reanalysis products.

Concerning the link between mTemp and the width of the distribution (STD), both regional models behave differently to the driving global simulations. In the regional simulations, the STD is negatively correlated with the mean temperature (s. Fig. 2a and

CPD
11, 1479–1518, 2015

c), indicating that colder periods tend to be related with a wider distribution of wind speed over the whole area. This is also supported by the negative correlation between mTemp and the difference P99 – P50 (not shown, Table 2). Since P50 was also negatively correlated with mTemp, the regional models tend to be associated with broader wind speed distributions and with stronger mean winds.

The two driving global simulations display, in contrast, positive correlations in a region along the North and South Baltic Sea, straddled by regions of zero or negative correlations in Scandinavia and central Europe (Fig. 2b and d).

We assume that this result may be induced by a stronger meridional temperature gradient (tGrad; see Sect. 3). This assumption is strengthened by the negative correlation between mTemp and tGrad, which shows a spatially averaged value of −0.56 in the CCLM simulation and −0.47 in the MM5 simulation. This negative correlation indicates that lower mean temperatures tend to occur with stronger meridional temperature gradients in these simulations, and thus, tGrad could be the primary driver for the changes in the wind speed distribution. Therefore, we also analysed the relationship between the parameters of the wind speed distribution and tGrad. This analysis reveals, however, contrasting results between both regional simulations: the correlations in the CCLM simulation are only minor and not statistically significant, whereas in the case of MM5 they are relatively strong for all parameters of the wind speed distribution, except for the difference P99 – P50.

We additionally investigate the relationship between the mean NAO index and the distribution of wind speeds. The correlation coefficient between the NAO index (see Sect. 3) and the median wind P50 displays clear similarities of the regional simulations and the driving global simulations, respectively (Fig. 3). However, the differences between the results provided by the regional models and those provided by the global models are profound. The correlation patterns derived from the regional models display positive correlations over oceanic areas, but in general negative correlations over land areas. This is reflected by a west–east correlation dipole (in the CCLM simulations the zero of this dipole does not coincide with the coast line). In contrast, the

CPD
11, 1479–1518, 2015

global simulations display positive correlations over the whole region (Fig. 3). The idea that a positive NAO index should be associated with stronger winds in general is only confirmed in the global simulations. The regional models indicate that a stronger NAO tends to be linked to stronger winds only over the ocean and coastal areas, but not over Central and Eastern Europe. This difference may hint to an influence of the boundary layer parametrization in regional models over continental areas.

The spatially averaged correlation between the NAO and STD is very low in the CCLM simulation (0.12), but much stronger and negative in the MM5 simulation (−0.42). This difference can now be explained by the different correlation patterns shown in Fig. 4a. The spatially resolved map showing the correlation between the NAO index and the grid-cell STD in the regional models CCLM and MM5 and in the global models ECHAM5 and ECHO-G is remarkably similar to the correlation patterns between the mean temperature and the STD (compare Figs. 4 and 2). Again, the CCLM simulation shows positive correlations over North Western Europe whereas the correlations in MM5 are negative over the whole region. The global models tend to show higher positive correlations over the North Sea and the Southern Baltic Sea, straddled by negative correlations over Scandinavia and Central Europe. Thus, the relationships between STD and the NAO and the relationship between STD and mTemp are similar, suggesting that both are a reflection of the same underlying physical phenomenon. However, this underlying link has a different spatial fingerprint in the regional models and in the global models.

4.3 The global model ECHAM6/MPIOM

ECHAM6 is so far the latest version of the series of atmospheric models including the atmospheric models ECHO-G (ECHAM4/HOPE-G) and ECHAM5. The simulation with ECHAM6 was conducted with a higher spatial resolution, T63 (approximately 1.875°) vs. T30/T31 (about 3.75°) for the other two ECHAM versions. In general the correlation patterns between the large-scale drivers and the parameters of the distribution of wind speed resemble those obtained with ECHAM5 and ECHO-G (ECHAM4/HOPE-G), but

CPD
11, 1479–1518, 2015

some clear differences exist. The higher spatial resolution of ECHAM6 does not, however, lead to correlation patterns that resemble those derived from the regional model simulations CCLM and MM5.

The correlation patterns between the median wind speed P50 and the mean temperature or the NAO index in ECHAM6 are indeed similar to the ones derived from ECHAM5 and ECHO-G, displaying generally positive, albeit weak, correlations between the median winds and temperature. The correlations between the median wind and the NAO index are positive and strong (Figs. 1 and 3). However, the correlations of these two driving factors with the width of the wind speed distribution, represented by STD, differ in ECHAM6 from the other two versions of ECHAM (Figs. 2 and 4). ECHAM6 displays correlation patterns that are positive and spatially more homogeneous, whereas the ECHAM5 and ECHO-G simulations show higher correlations in the Southern Baltic surrounded by negative correlations in Scandinavia and Central Europe. Physically, the relationship between mTemp and median wind is positive but statistically not significant in the ECHAM6 simulation. This indicates that warmer temperatures are accompanied by a shift towards higher wind speeds and by a slight tendency to a broader wind speed distribution (see also Fig. 2e). tGrad shows negative correlation with the median wind, consistent with the link between a decreased temperature gradient in warmer periods (see also Fig. 4e).

4.4 The reanalysis data coastDat2 and NCEP

We present the link between the large-scale drivers and the wind speed distribution for the two reanalysis products NCEP and coastDat2. It can be argued that these two reanalysis data sets should be closer to the real climate, because they both incorporate information based on meteorological observations. On the other hand, the reanalysis models are integrated over a relatively short period of time of about 60 years. Therefore the decadal-scale links between the large-scale climate drivers and the probability distribution of wind speed derived from these data sets is most likely afflicted with a higher degree of uncertainty. The correlation patterns derived from NCEP and coastDat2 are

CPD
11, 1479–1518, 2015

based on gliding 5 year windows, instead of 30 year windows as for the longer simulations described before.

The correlation between mTemp and the parameters of the wind speed distribution for coastDat2 and NCEP shows generally significant positive values with P50, STD, P95 and P99, but no significant correlation for diffM and diffE. The spatially resolved correlation between mTemp and P50 and the STD field is also dominated by positive values, with highest coefficients over southern Norway, and weaker or slightly negative correlations in the southern regions of the domain (s. Figure 2f). Therefore, the correlation patterns in the reanalysis data represent a shift of the wind speed distribution from low to high wind speeds during warmer periods, with a tendency to wider wind speed distribution in the northern and a small influence of temperature in the southern regions.

The relationship between tGrad and mTemp is negative (−0.25 for coastDat2, −0.52 for NCEP), again showing that colder periods are related to stronger meridional temperature gradients in agreement with all other models analysed here. Thus, the results obtained from the reanalysis products resemble more closely the ones derived from the global climate model simulations (ECHAM5, ECHAM6, ECHO-G) than from the regional simulations (MM5 and CCLM).

The correlation between tGrad and the distribution of wind speed is found to be predominantly weak in the coastDat2 data, with the only statistically significant value (0.34) for the correlation tGrad-diffM. This result means that higher temperature differences between North and South are slightly correlated with a broader wind speed distribution. In contrast, for the NCEP reanalysis, the link is strong but opposite: weaker meridional gradients are linked to stronger median winds and wider wind speed distributions.

Regarding the link to the NAO, both reanalysis data sets display a consistent picture, with a positive NAO closely linked to stronger median winds and wider distributions (STD) in most of the domain. This link is stronger over the northern regions and becomes smaller and even negative over the southern fringes of the domain. Again, this

CPD
11, 1479–1518, 2015

spatial structure resembles more closely the structure provided by the global models and differs from the pattern provided by the regional models.

4.5 Centennial-scale evolution of the wind speed variance over the past millennium

In the previous sections we analysed the links between large-scale atmospheric drivers and the distribution of wind speed. The time series of the width of the wind speed distribution over the past millennium indicate, however, that the slowly changing soil boundary conditions may also have a strong influence on the long-term evolution of the variability of wind speed in Northern Europe. Figure 6a shows the time series of the spatially averaged STD of the wind speed distribution at each model grid-cell for the simulation conducted with the model ECHAM6. The most remarkable feature of the averaged STD is its almost continuous increase during the simulated period. It does not show an obvious relationship with the evolution of the spatially averaged temperature at these long time scales (Fig. 5). This monotonous increase is also seen in the corresponding time series calculated with the output of the ECHAM5 simulation (not shown), but not in the data of the ECHO-G (based on ECHAM4) simulation (Fig. 6b). A suggestion about the origin of the increase in the STD of the wind speed distribution can be obtained by comparing the spatially resolved STD in the last decades vs. the initial decades in the simulation. Figure 7a shows the ratio between the spatially resolved STD for the periods 1871–1990 AD and 1001–1091 AD, respectively. The values of this ratio are higher than unity (STD larger at the end of the simulation) over the land areas of central Europe, with a maximum at about 25° E. The STD over oceanic grid-cells and over Scandinavia does not change significantly between these two periods in the simulations. Again, this spatial pattern of increase in the width of the wind speed distribution is also simulated by the ECHAM5 simulation (not shown), but not in ECHO-G where the ratio is scattered around 1 (not shown).

The spatial pattern of changes in STD between the beginning and end of the ECHAM6 and ECHAM5 simulation suggests that the increase in the width of the wind

CPD
11, 1479–1518, 2015

speed distribution may be related to surface-boundary processes. This suggestion is supported by the changes in forest cover in the course of the last millennium as reconstructed by Pongratz et al. (2008). This reconstruction was used to drive the models ECHAM6 and ECHAM5 (see Sect. 2). The difference in tree fraction in each model grid-cell between the periods 1871–1990 AD and 1001–1091 AD is shown in Fig. 7b. The spatial agreement between the reduction in tree fraction and the widening of the wind speed distribution between the beginning and the end of the millennium is remarkable and strongly supports the hypothesis that the distribution of wind speed is mainly affected by land-use changes and related changes in surface roughness length. A less extensive forest cover causes a widening of the wind speed distribution, and vice versa. The simulation with the model ECHO-G, which was not driven by changes in land use, does not show a long-term increase or change in the width of the distribution of wind speeds, supporting the strong influence of land cover changes on the distribution of wind speeds.

Therefore, at centennial timescales the correlation between the wind speed distribution and temperature that was explored in the previous sections could have been indirectly caused by land-use changes. At these timescales, anthropogenic deforestation and mean temperature exhibit a positive trend. Thus the expansion of the wind speed distribution and the increase of temperature in these decades might be induced by physically different factors, leading to positive correlations in our analysis. This statistical effect can be disentangled by separating the analysis of these simulations into two parts (P1: years 850–1500 AD, P2: years 1500–2005 AD). The correlations between mean temperature and the width of the wind distribution does show a difference in the correlation. For P1 of ECHAM6 mTemp-diffM is around 0 and mTemp-diffE −0.25, for P2 0.63 and 0.57, respectively. For P1 of ECHAM5 mTemp-diffM is −0.26 and mTemp-diffE is −0.38, for P2 0.26 and 0.12, respectively. Both parts in the GCMs show different signs for the relation between mean temperature and the shape of the wind speed distribution. These results suggest that specifically for ECHAM6 the correlation between

CPD
11, 1479–1518, 2015

the mean temperature and the width of the wind speed distribution is a statistical artifact mediated by deforestation.

5 Discussion and conclusions

This study investigates and compares different simulation data sets and reanalysis products, on time scales covering the last decades to the past millennium, regarding the probability distribution of the daily wind speed in winter time over Northern Europe. Our investigation is aimed at identifying the large-scale factors that drive changes in this probability distribution. The study is based on correlations between different parameters of the wind speed distribution and different climatic indices related to mean temperature, meridional temperature gradient and the North Atlantic Oscillation. The overlaying question is whether and how the wind speed distribution may change during varying climate conditions and hence whether these conditions may provoke more and/or stronger wind speed extremes.

One prominent result is that the link between the thermal indices and the North Atlantic Oscillation appears physical consistent in all data sets, and thus all models are consistent in this regard. The relationship between the NAO and mean temperature in wintertime is positive in all models, as this is caused by the advection of maritime air masses by stronger westerly winds in a more positive NAO state. Also, the correlation between mean Temperature (mTemp) and the temperature gradient (tGrad) shows negative values for all models, indicating that warmer periods are linked to a weakened meridional temperature gradient. This might be explained by the fact that northern regions warm (cool) more strongly when the overall temperature is higher (lower). In climate change projections this is referred to as polar amplification, although it has been also identified in paleoclimate simulations and reconstructions over the past millennium (Luterbacher et al., 2002).

However, a second important result is that the correlation between the large-scale indices and the parameters of the wind speed distribution exhibit markedly different

CPD
11, 1479–1518, 2015

results among the data sets analysed and it is difficult to derive general conclusions on the effect of these large-scale drivers on the distribution of daily wind.

Nevertheless, the three global simulations present similarities that warrant to place them in one group. Figure 1 through 4 show patterns of correlations obtained in the global simulations that are generally similar. This can be expected to a certain degree because the three atmospheric models included in the GCM belong to the same ECHAM family. Likewise, the correlation patterns obtained from the two regional models are also generally similar, although in this case both models, MM5 and CCLM, are structurally different.

The striking result is that the regional models do not seem to inherit the dynamical properties of their respective global models, but produce instead different correlation patterns between the large-scale drivers and the wind speed distributions. In the case of the link between the median wind and the large-scale drivers, the differences between each regional model and its driving global model mostly occur over land areas (see Figs. 1 and 3). However, in case of the link between the STD of wind speed and the large-scale drivers, the differences seem spatially more complex. It is plausible that the higher resolution and the different parametrization schemes of the boundary layer shape the link between the large-scale dynamics and turbulent processes that modulate the width of the daily wind distribution.

The comparison of the correlation coefficients in Table 2 shows differences in signs and statistical significance. Regarding statistical significance, it is noticeable that for tGrad and wind speed there are only significant values for MM5 and NCEP, although with different signs. CCLM as one of the regional model simulations is the only simulation which shows no significant correlations. Its forcing global model ECHAM5 only shows significance for the NAO–wind speed correlation. ECHAM6 as the successor of ECHAM5 also shows only significant values for tGrad–mTemp and for NAO–wind. ECHO-G and coastDat2 show significant values only for wind speed values in correlation with mTemp.

CPD
11, 1479–1518, 2015
Variability of wind speed distribution during the past millennium
S. E. Bierstedt et al.

The correlation between tGrad and wind speed shows significant values only for MM5 and NCEP but both data sets exhibit different signs. MM5 reveals positive correlations, which implies that stronger winds are associated with a stronger temperature gradient. This positive correlation is only appreciated for the regional data sets: MM5, CCLM and coastDat2. The global data sets, ECHO-G, ECHAM5, ECHAM6 and NCEP, show negative values, indicating stronger winds corresponding to weaker temperature gradients. These results demonstrate that the influence of the spatial resolution and the different boundary layer parametrization may be a critical factor to establish a link between climate change and changes in near-surface wind speeds.

Another indicator for the influence of the spatial resolution on our results might be the fact that only the regional simulations MM5 and CCLM show negative correlations between mean temperature and the width of the probability distribution as measured by diffM/diffE. These correlations suggest that colder periods are connected with stronger wind speed extremes. In contrast, the GCM data show no clear correlations between these parameters. This study does not allow us to provide a comprehensive dynamical explanation for the different behavior of wind speeds in changing temperature or pressure conditions: the models show different results although each model seems to be dynamical consistent in itself. Therefore, a detailed analysis of each of the simulations, and maybe of the computer codes, seems required to understand how the different correlation patterns arise.

On centennial timescales, we identified land-use changes as a very important factor modulating near-surface wind in the simulations. Note that anthropogenic changes in land-use are prescribed only in the ECHAM5 and ECHAM6 simulations, whereas for ECHO-G land-use is kept constant during the whole simulation. The analysis of the ECHAM5 and ECHAM6 millennium simulations reveals a strong increase of the STD of wind speed for the last decades since the industrialization, and in areas that coincide with larger deforestation along the last centuries. The impact of land-use changes on wind conditions was also shown by Pessacg and Solman (2013) in simulations with the regional model MM5 over South America for different idealized land-use scenarios.

The main conclusion that can be drawn from this study is that the link between large-scale climate drivers and the distribution of daily wind speeds in wintertime in this region is complex. All models analysed here have been individually profusely used in climate simulations and the data sets have been used in a number of other previous studies, and no gross deficiencies have been pointed out so far. Our study is different because of the long paleo-simulation (e.g. MM5, which is rather used as a short time prediction model), and the comparison of all these models regarding a relationship between temperature and NAO conditions and wind speed. We conclude that, although climate models may be dynamically sound in the large-scale contest, the impact of climate change on variables like near-surface wind speed distribution possibly depends more strongly on the details of the physical parametrization and changes in surface forcing, like deforestation, than on the large-scale dynamical drivers, such as large-scale temperature or sea-level-pressure changes.

Acknowledgements. This work is a contribution to the Helmholtz Climate Initiative REKLIM (Regional Climate Change), a joint research project of the Helmholtz Association of German Research Centres (HGF). The MM5 simulation was carried within the SPEQTRES project (Spanish Ministry of Economy and Competitiveness, ref. CGL2011-29672-C02-02). The work benefited from the Cluster of Excellence “CliSAP” (EXC177), Universität Hamburg, funded through the German Research Foundation (DFG).

The article processing charges for this open-access publication were covered by a Research Centre of the Helmholtz Association.

References

2k Consortium, P.: Continental-scale temperature variability during the past two millennia, Nat. Geosci., 6, 339–346, 2013. 1483

Brönnimann, S., Martius, O., von Waldow, H., Welker, C., Luterbacher, J., Compo, G., Sardeshmukh, P., and Usbeck, T.: Extreme winds at northern mid-latitudes since 1871, Meteorol. Z., 21, 013–027, 2012. 1482

CPD

11, 1479–1518, 2015

Variability of wind speed distribution during the past millennium

S. E. Bierstedt et al.

Compo, G. P., Whitaker, J. S., Sardeshmukh, P. D., Matsui, N., Allan, R. J., Yin, X., Gleason, B. E., Vose, R. S., Rutledge, G., Bessemoulin, P., Brönnimann, S., Brunet, M., Crouthamel, R. I., Grant, A. N., Groisman, P. Y., Jones, P. D., Kruk, M. C., Kruger, A. C., Marshall, G. J., Maugeri, M., Mok, H. Y., Nordli, O., Ross, T. F., Trigo, R. M., Wang, X. L., Woodruff, S. D., and Worley, S. J.: The twentieth century reanalysis project, Q. J. Roy. Meteor. Soc., 137, 1–28, 2011. 1482

Costas, I.: Climate Archive Dune, Ph.D. thesis, Hamburg University, 2013. 1481, 1483

Crowley, T. J., Zielinski, G., Vinther, B., Udisti, R., Kreutz, K., Cole-Dai, J., and Castellano, J.: Volcanism and the little ice age, PAGES Newsletter, 16, 22–23, 2008. 1486

Crueger, T., Stevens, B., and Brokopf, R.: The Madden–Julian oscillation in ECHAM6 and the introduction of an objective mjo metric, J. Climate, 26, 3241–3257, 2013. 1486

Doms, G., J. F., Heise, E., Herzog, H.-J., Mrionow, D., Raschendorfer, M., Reinhart, T., Ritter, B., Schrodin, R., Schulz, J.-P., and Vogel, G.: A description of the nonhydrostatic regional cosmo model. Part ii: Physical parameterization, Technical report, Deutscher Wetterdienst, 2011. 1487

Donnelly, J. P. and Woodruff, J. D.: Intense hurricane activity over the past 5,000 years controlled by el niño and the west african monsoon, Nature, 447, 465–468, 2007. 1482

Ebisuzaki, W.: A method to estimate the statistical significance of a correlation when the data are serially correlated, J. Climate, 10, 2147–2153, 1997. 1489

Esper, J., Düthorn, E., Krusic, P., Timonen, M., and Büntgen, U.: Northern European summer temperature variations over the common era from integrated tree-ring density records, J. Quaternary Sci., 29, 487–494, 2014. 1483

Fernández-Donado, L., González-Rouco, J. F., Raible, C. C., Ammann, C. M., Barriopedro, D., García-Bustamante, E., Jungclaus, J. H., Lorenz, S. J., Luterbacher, J., Phipps, S. J., Servonnat, J., Swingedouw, D., Tett, S. F. B., Wagner, S., Yiou, P., and Zorita, E.: Large-scale temperature response to external forcing in simulations and reconstructions of the last millennium, Clim. Past, 9, 393–421, doi:10.5194/cp-9-393-2013, 2013. 1483

Feser, F., Rockel, B., von Storch, H., Winterfeldt, J., and Zahn, M.: Regional climate models add value to global model data: a review and selected examples, B. Am. Meteorol. Soc., 92, 1181–1192, 2011. 1484

Feser, F., Barcikowska, M., Krueger, O., Schenk, F., Weisse, R., and Xia, L.: Storminess over the North Atlantic and Northwestern Europe – a review, Q. J. Roy. Meteor. Soc., 141, 350–382, 2014. 1482

CPD
11, 1479–1518, 2015

Variability of wind speed distribution during the past millennium

S. E. Bierstedt et al.

Fischer-Bruns, I., von Storch, H., Gonzalez-Rouco, J. F., and Zorita, E.: Modelling the variability of midlatitude storm activity on decadal to century time scales, Clim. Dynam., 25, 461–476, 2005. 1483

Geyer, B.: High-resolution atmospheric reconstruction for Europe 1948–2012: coastDat2, Earth Syst. Sci. Data, 6, 147–164, doi:10.5194/essd-6-147-2014, 2014. 1487

Gillett, N. P. and Fyfe, J. C.: Annular mode changes in the cmip5 simulations, Geophys. Res. Lett., 40, 1189–1193, 2013. 1482

Giorgetta, M. A., Jungclaus, J., Reick, C. H., Legutke, S., Bader, J., Böttinger, M., Brovkin, V., Crueger, T., Esch, M., Fieg, K., Glushak, K., Gayler, V., Haak, H., Hollweg, H.-D., Ilyina, T., Kinne, S., Kornblueh, L., Matei, D., Mauritsen, T., Mikolajewicz, U., Mueller,W., Notz, D., Pithan, F., Raddatz, T., Rast, S., Redler, R., Roeckner, E., Schmidt, H., Schnur, R., Segschneider, J., Six, K. D., Stockhause, M., Timmreck, C., Wegner, J., Widmann, H., Wieners, K.-H., Claussen, M., Marotzke, J., and Stevens, B.: Climate and carbon cycle changes from 1850 to 2100 in MPI-ESM simulations for the coupled model intercomparison project phase 5, J. Adv. Model. Earth Syst., 5, 572–597, 2013 1486

Gómez-Navarro, J. J. and Zorita, E.: Atmospheric annular modes in simulation over the past millennium: no long-term response to external forcing, Geophys. Res. Lett., 40, 3232–3236, 2013. 1482

Gómez-Navarro, J. J., Montávez, J. P., Wagner, S., and Zorita, E.: A regional climate palaeosimulation for Europe in the period 1500–1990 – Part 1: Model validation, Clim. Past, 9, 1667–1682, doi:10.5194/cp-9-1667-2013, 2013. 1487

Gómez-Navarro, J. J., Bothe, O., Wagner, S., Zorita, E., Werner, J. P., Luterbacher, J., Raible, C. C., and Montávez, J. P.: A regional climate palaeosimulation for Europe in the period 1501–1990 – Part II: Comparison with gridded reconstructions, Clim. Past Discuss., 11, 307–343, doi:10.5194/cpd-11-307-2015, 2015. 1487

Hall, A.: Projecting regional change, Science, 346, 1461–1462, 2014. 1484

Hall, A. and Qu, X.: Using the current seasonal cycle to constrain snow albedo feedback in future climate change, Geophys. Res. Lett., 33, L03502, doi:10.1029/2005GL025127, 2006. 1490

Hong, S.-Y. and Pan, H.-L.: Nonlocal boundary layer vertical diffusion in a medium-range forecast model, Mon. Weather Rev., 124, 2322–2339, 1996. 1487

Hünicke, B., Zorita, E., and Haeseler, S.: Holocene climate simulations for the baltic sea region – application for sea level and verification of proxy data, Berichte der RGK, 92, 211–249, 2011. 1485

Hunt, B.: The medieval warm period, the little ice age and simulated climatic variability, Clim. Dynam., 27, 677–694, 2006. 1483

Jungclaus, J. H., Lorenz, S. J., Timmreck, C., Reick, C. H., Brovkin, V., Six, K., Segschneider, J., Giorgetta, M. A., Crowley, T. J., Pongratz, J., Krivova, N. A., Vieira, L. E., Solanki, S. K., Klocke, D., Botzet, M., Esch, M., Gayler, V., Haak, H., Raddatz, T. J., Roeckner, E., Schnur, R., Widmann, H., Claussen, M., Stevens, B., and Marotzke, J.: Climate and carbon-cycle variability over the last millennium, Clim. Past, 6, 723–737, doi:10.5194/cp-6-723-2010, 2010. 1486

Kalnay, E., Kanamitsu, M., Kistler, R., Collins, W., Deaven, D., Gandin, L., Iredell, M., Saha, S., White, G., Woollen, J., Zhu, Y., Leetmaa, A., Reynolds, R., Chelliah, M., Ebisuzaki, W., Higgins, W., Janowiak, J., Mo, K. C., Ropelewski, C., Wang, J., Jenne, R., and Joseph, D.: The NCEP/NCAR 40-Year Reanalysis Project, B. Am. Meteorol. Soc., 77, 437–471, 1996. 1487

Kistler, R., Kalnay, E., Collins, W., Saha, S., White, G., Woollen, J., Chelliah, M., Ebisuzaki, W., Kanamitsu, M., Kousky, V., van den Dool, H., Jenne, R., and Fiorino, M.: The NCEP/NCAR 50-Year Reanalysis: monthly means cd-rom and documentation, B. Am. Meteorol. Soc., 82, 247–267, 2001. 1487

Krivova, N. and Solanki, S.: Models of solar irradiance variations: current status, J. Astrophys. Astron., 29, 151–158, 2008. 1486

Krueger, O., Schenk, F., Feser, F., and Weisse, R.: Inconsistencies between long-term trends in storminess derived from the 20CR reanalysis and observations, J. Climate, 26, 868–874, 2013. 1482

Legutke, S. and Voss, R.: The Hamburg atmosphere–ocean coupled circulation model echo-g, Technical Report 18, DKRZ, Hamburg, 1999. 1485

Li, M. and Woollings, T.: Extratropical cyclones in a warmer, moister climate: a recent atlantic analogue, Geophys. Res. Lett., 41, 8594–8601, 2014. 1481

Luterbacher, J., Xoplaki, E., Dietrich, D., Rickli, R., Jacobeit, J., Beck, C., Gyalistras, D., Schmutz, C., and Wanner, H.: Reconstruction of sea level pressure fields over the eastern north atlantic and Europe back to 1500, Clim. Dynam., 18, 545–561, 2002. 1490, 1501

CPD
11, 1479–1518, 2015

Variability of wind speed distribution during the past millennium

S. E. Bierstedt et al.

Luterbacher, J., Dietrich, D., Xoplaki, E., Grosjean, M., and Wanner, H.: European seasonal and annual temperature variability, trends, and extremes since 1500, Science, 303, 1499–1503, 2004. 1483

Marsland, S. J., Haak, H., Jungclaus, J. H., Latif, M., and Roeske, F.: The max planck institute global ocean/sea ice model with orthogonal curvilinear coordinates, Ocean Model., 5, 91–127, 2003. 1486

Pessacg, N. L. and Solman, S.: Effects of land-use changes on climate in southern south america, Clim. Res., 55, 33–51, 2013. 1503

Pithan, F. and Mauritsen, T.: Arctic amplification dominated by temperature feedbacks in contemporary climate models, Nat. Geosci., 7, 181–184, 2014. 1490

Pongratz, J., Reick, C., Raddatz, T., and Claussen, M.: A reconstruction of global agricultural areas and land cover for the last millennium, Global Biogeochem. Cy., 22, GB3018, doi:10.1029/2007GB003153, 2008. 1486, 1500, 1518

Rockel, B. W. and Hense, A.: The regional climate model Cosmo-CLM (CCLM), Meteorol. Z., 12, 347–348, 2008. 1487

Roeckner, E., Arpe, K., Bengtsson, L., Christoph, M., Claussen, M., Dümenil, L., Esch, M., Giorgetta, M., Schlese, U., and Schulzweida, U.: The atmospheric general circulation model ECHAM4: model description and simulation of present-day climate, Technical Report 218, MPI-M, Hamburg, 1996. 1485

Roeckner, E., Bäuml, G., Bonaventura, L., Brokopf, R., Esch, M., Giorgetta, M., Hagemann, S., Kirchner, I., Kornblueh, L., Manzini, E., Rhodin, A., Schlese, U., Schulzweida, U., and Tompkins, A.: The atmospheric general circulation model ECHAM5. Part I: Model description, Technical Report 349, Max Planck Institute for Meteorology, Hamburg 2003. 1485

Schimanke, S., Meier, H. E. M., Kjellström, E., Strandberg, G., and Hordoir, R.: The climate in the Baltic Sea region during the last millennium simulated with a regional climate model, Clim. Past, 8, 1419–1433, doi:10.5194/cp-8-1419-2012, 2012. 1483

Schreiber, T. and Schmitz, A.: Improved surrogate data for nonlinearity tests, Phys. Rev. Lett., 77, 635, doi:10.1103/PhysRevLett.77.635, 1996. 1489

Seneviratne, S., Nicholls, N., Easterling, D., Goodess, C., Kanae, S., Kossin, J., Luo, Y., Marengo, J., McInnes, K., Rahimi, M., Reichstein, M., Sorteberg, A., Vera, C., and Zhang, X.: Changes in climate extremes and their impacts on the natural physical environment, in: Managing the Risks of Extreme Events and Disasters to Advance Climate Change Adaptation, edited by: Field, C. B., Barros, V., Stocker, T. F., Qin, D., Dokken, D. J., Ebi, K. L., Mastrandrea, M. D., Mach, K. J., Plattner, G.-K., Allen, S. K., Tignor, M., and Midgley, P. M., a special report of working groups I and II of the Intergovernmental Panel on Climate Change (IPCC), Technical report, Cambridge University Press, Cambridge, UK, New York, NY, USA, 109–230, 2012. 1481

Stevens, B., Giorgetta, M., Esch, M., Mauritsen, T., Crueger, T., Rast, S., Salzmann, M., Schmidt, H., Bader, J., Block, K., Brokopf, R., Fast, I., Kinne, S., Kornblueh, L., Lohmann, U., Pincus, R., Reichler, T., and Roeckner, E.: Atmospheric component of the MPI-M earth system model: ECHAM6, J. Adv. Model. Earth Syst., 5, 146–172, 2013. 1486

Taylor, K. E., Stouffer, R. J., and Meehl, G. A.: An overview of CMIP5 and the experiment design, B. Am. Meteorol. Soc., 93, 485–498, 2012. 1486

von Storch, H., Langenberg, H., and Feser, F.: A spectral nudging technique for dynamical downscaling purposes, Mon. Weather Rev., 128, 3664–3673, 2000. 1487

von Storch, H., Zorita, E., Jones, J., Dimitriev, Y., González-Rouco, F., and Tett, S.: Reconstructing past climate from noisy data, Science, 306, 679–682, 2004. 1485

Wang, X. L., Feng, Y., Compo, G. P., Zwiers, F. W., Allan, R. J., Swail, V. R., and Sardeshmukh, R. D.: Is the storminess in the twentieth century reanalysis really inconsistent with observations? A reply to the comment by Krueger et al. (2013), Clim. Dynam., 42, 1113–1125, 2013. 1482

Wolff, J., Maier-Reimer, E., and Legutke, S.: The Hamburg Primitive Equation Model HOPE, Technical Report 8, Germany Climate Computer Center (DKRZ), Hamburg, 1997. 1485

Yin, J. H.: A consistent poleward shift of the storm tracks in simulations of 21st century climate, Geophys. Res. Lett., 32, L18701, doi:10.1029/2005GL023684, 2005. 1481

Zorita, E., von Storch, H., Gonzalez-Rouco, J. F., Cubasch, U., Luterbacher, J., Legutke, S., Fischer-Bruns, I., and Schlese, U.: Climate evolution in the last five centuries simulated by an atmosphere–ocean model: global temperatures, the north atlantic oscillation and the late maunder minimum, Meteorol. Z., 13, 271–289, 2004. 1485

CPD
11, 1479–1518, 2015

Table 1. Overview of the analysed simulations/reanalysis and their simulation acronyms, underlying atmosphere and ocean models, boundary forcings (only for regional data sets) as well as the spatial resolution of the atmosphere models and time periods, as used for the analysis.

	Simulation	Atmosphere	Ocean	Boundary	atm. spatial res.	Vegetation	Period
GCM	ECHO-G	ECHAM4	HOPE-G		3.75°	constant	1001–1990
	ECHAM5	ECHAM5	MPI-OM		3.75°	time dependent	850–2005
	ECHAM6	ECHAM6	MPI-OM		3.75°	time dependent	850–2005
RCM	MM5	MM5		ECHO-G	0.5°	constant	1001–1990
	CCLM	CCLM		ECHAM5	0.5°	constant	1655–1999
Reanalysis	coastDat2	CCLM*		NCEP	0.22°	constant	1948–2012
	NCEP				2.5°	constant	1948–2012

* with spectral nudging.

CPD
11, 1479–1518, 2015

Variability of wind speed distribution during the past millennium

S. E. Bierstedt et al.

Table 2. Time correlation coefficients between the following parameters of the probability distribution of daily mean wind speed: STD of wind speed, the 50th, 95th and 99th percentile (P50, P95, P99) and the differences between P95 – P50 (diffM) and P99 – P95 (diffE) and some large-scale drivers: spatially averaged December–February air temperature (mTemp), the spatial air temperature gradient (tGrad) and the North Atlantic Oscillation index (NAO). The parameters of the probability distributions have been computed in 30 year sliding windows for the simulations and in 5 year sliding windows for the reanalysis products. The time series of the drivers have been smoothed with a running mean filter. Significant coefficients (tested with a random phased bootstrap method) are written in bold.

	MM5	CCLM	ECHO-G	ECHAM5	ECHAM6	coastDat2	NCEP
tGrad – mTemp	**−0.47**	−0.56	**−0.35**	−0.24	**−0.53**	−0.25	**−0.52**
mTemp – STD	**−0.76**	−0.26	0.34	0.22	0.34	**0.40**	**0.36**
mTemp – P50	**−0.40**	0.15	**0.74**	0.41	0.43	**0.72**	**0.76**
mTemp – P95	**−0.79**	−0.18	**0.60**	0.31	0.37	**0.53**	**0.52**
mTemp – P99	**−0.79**	−0.30	**0.54**	0.24	0.34	**0.43**	**0.37**
mTemp – diffM	**−0.75**	−0.43	0.04	0.13	0.26	0.01	0.05
mTemp – diffE	**−0.67**	−0.34	0.11	−0.06	0.18	0	**−0.38**
tGrad – STD	**0.45**	0.13	−0.01	−0.08	−0.38	0.23	−0.27
tGrad – P50	**0.40**	0.10	−0.13	−0.08	−0.42	−0.05	**−0.48**
tGrad – P95	**0.52**	0.21	−0.05	−0.07	−0.38	0.17	**−0.35**
tGrad – P99	**0.45**	0.15	−0.16	−0.08	−0.36	0.14	**−0.34**
tGrad – diffM	**0.44**	0.20	0.10	−0.05	−0.31	0.34	−0.08
tGrad – diffE	0.26	0	−0.28	−0.08	−0.18	0	0.01
NAO – STD	**−0.42**	0.12	**0.34**	**0.37**	**0.44**	**0.70**	**0.58**
NAO – P50	**−0.12**	0.67	**0.64**	**0.54**	**0.52**	**0.86**	**0.80**

CPD
11, 1479–1518, 2015

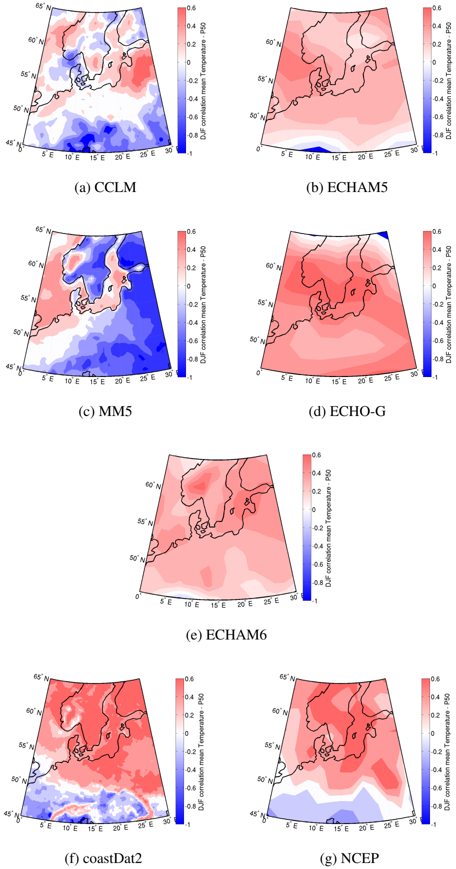

Figure 1. Field correlation of mean temperature and 50th percentile of wind speed for 7 different data sets: **(a)** CCLM (1655–1999 AD), **(b)** ECHAM5 (850–2005 AD), **(c)** MM5 (1001–1990 AD), **(d)** ECHO-G (1001–1990 AD), **(e)** ECHAM6 (850–2005 AD), **(f)** coastDat2 (1948–2012 AD), **(g)** NCEP (1948–2012 AD).

CPD
11, 1479–1518, 2015

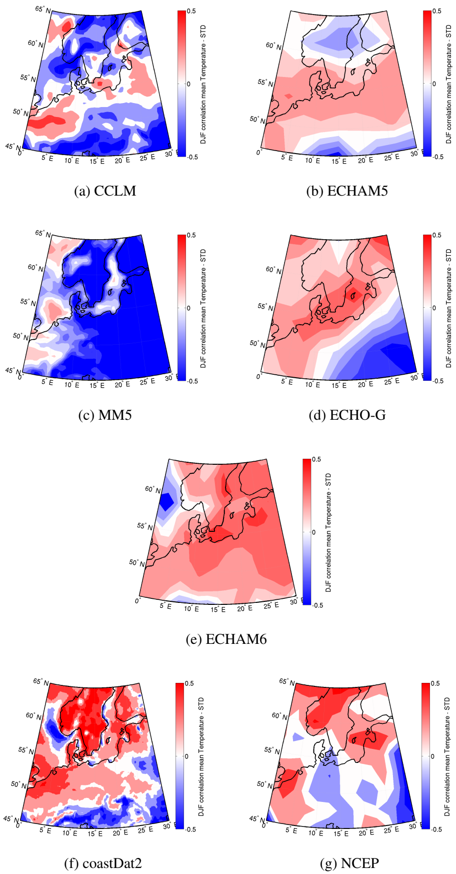

Figure 2. Field correlation between mean temperature and STD of wind speed for 7 different data sets: **(a)** CCLM (1655–1999 AD), **(b)** ECHAM5 (850–2005 AD), **(c)** MM5 (1001–1990 AD), **(d)** ECHO-G (1001–1990 AD), **(e)** ECHAM6 (850–2005 AD), **(f)** coastDat2 (1948–2012 AD), **(g)** NCEP (1948–2012 AD).

CPD
11, 1479–1518, 2015

S. E. Bierstedt et al.

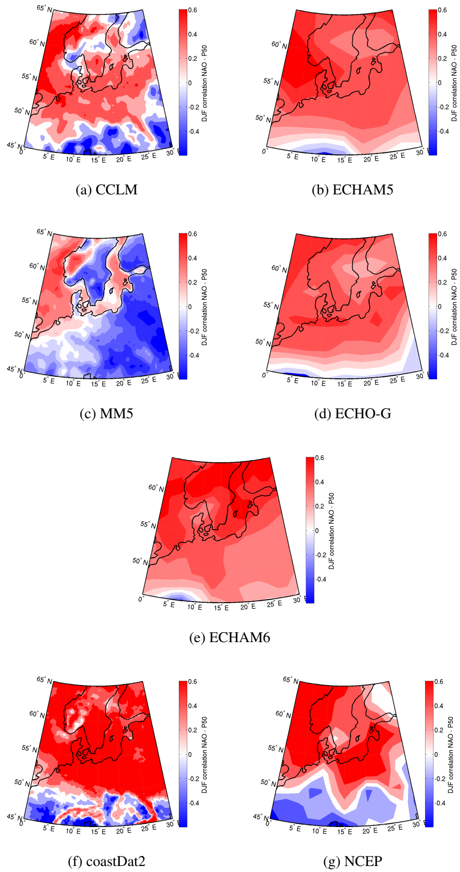

Figure 3. Field correlation between NAO and 50th percentile of wind speed for 7 different data sets: **(a)** CCLM (1655–1999 AD), **(b)** ECHAM5 (850–2005 AD), **(c)** MM5 (1001–1990 AD), **(d)** ECHO-G (1001–1990 AD), **(e)** ECHAM6 (850–2005 AD), **(f)** coastDat2 (1948–2012 AD), **(g)** NCEP (1948–2012 AD).

CPD
11, 1479–1518, 2015

Title Page
Abstract | Introduction
Conclusions | References
Tables | Figures
◀| |▶
◀ ▶
Back | Close
Full Screen / Esc
Printer-friendly Version
Interactive Discussion

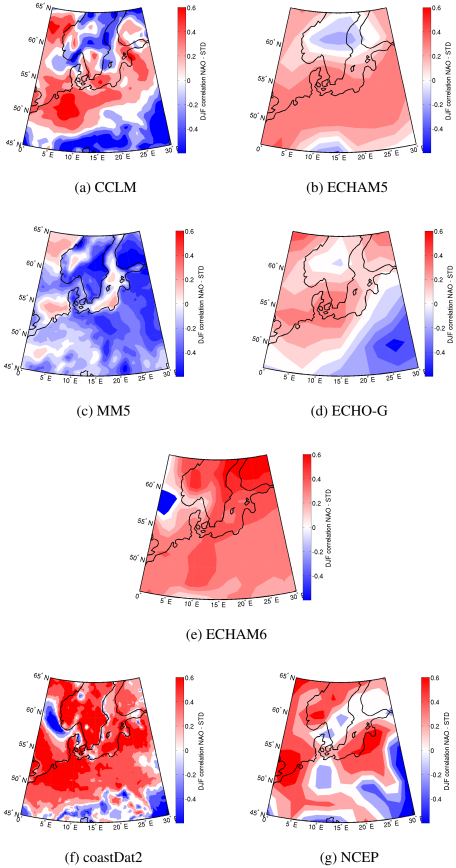

Figure 4. Field correlation between NAO and STD of wind speed for 7 different data sets: **(a)** CCLM (1655–1999 AD), **(b)** ECHAM5 (850–2005 AD), **(c)** MM5 (1001–1990 AD), **(d)** ECHO-G (1001–1990 AD), **(e)** ECHAM6 (850–2005 AD), **(f)** coastDat2 (1948–2012 AD), **(g)** NCEP (1948–2012 AD).

CPD
11, 1479–1518, 2015

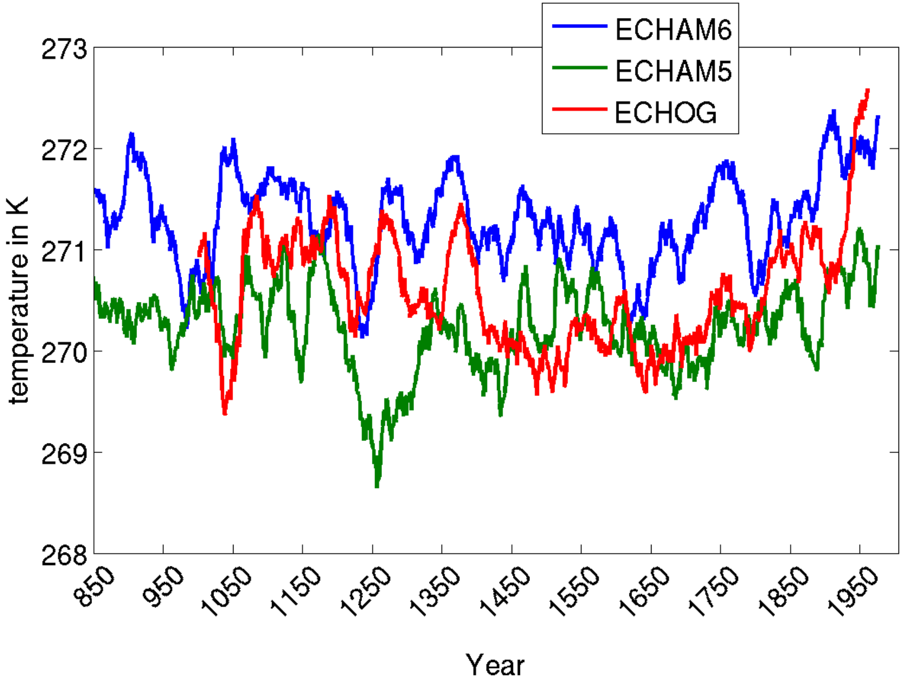

Figure 5. Comparison of yearly mean temperature for ECHAM6 (blue), ECHAM5 (green) and ECHO-G (red).

CPD
11, 1479–1518, 2015

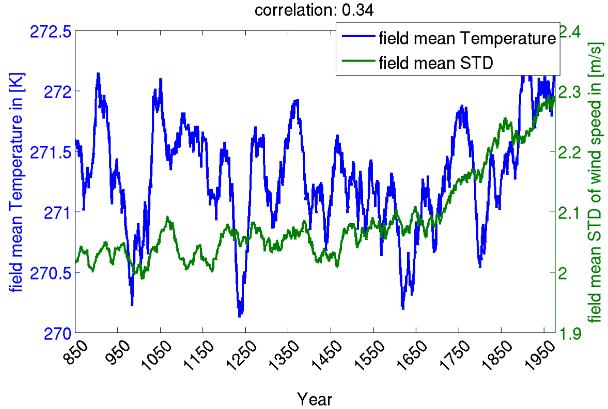

a)

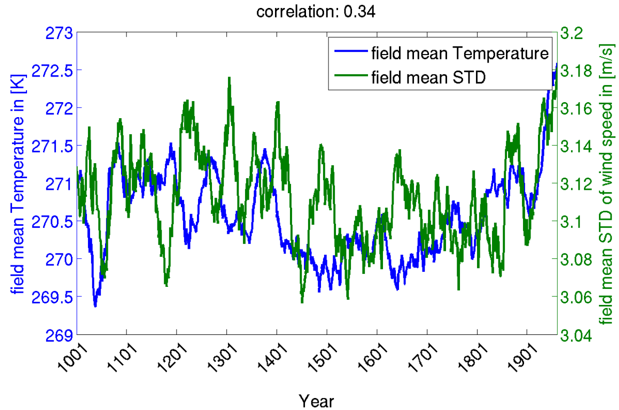

b)

Figure 6. Time series of yearly mean temperature (blue) and the STD of the wind speed (green) for the GCMs ECHAM6 **(a)** and ECHO-G **(b)**. In both models the correlation between the blue and the green line is 0.34.

CPD
11, 1479–1518, 2015

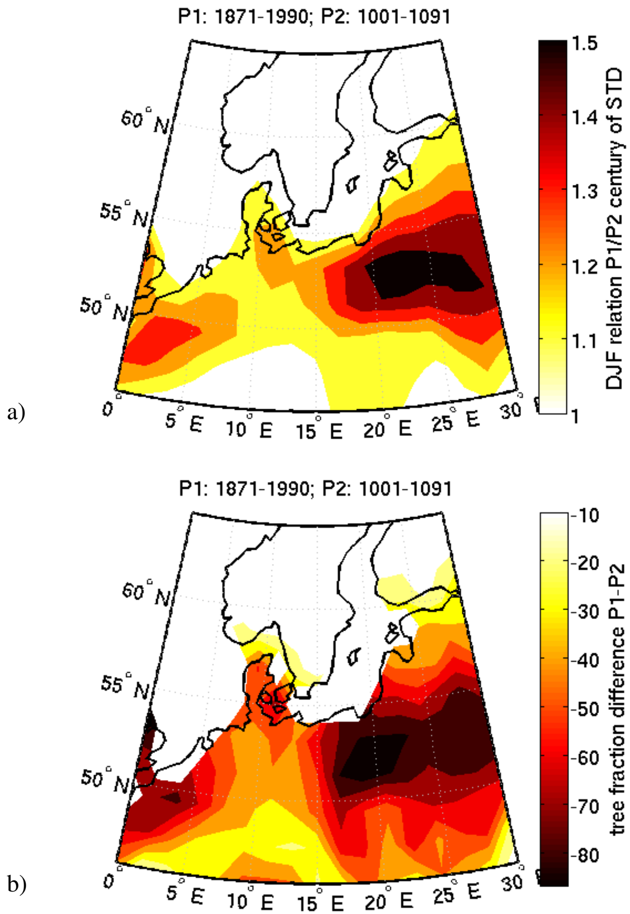

Figure 7. (a) Relation between part 1 (P1: 1871–1990) and part 2 (P2: 1001–1091) STD of wind speed (ECHAM6). **(b)** Tree fraction difference of P1 minus P2 derived from Pongratz et al. (2008).